IOSR Journal of Dental and Medical Sciences (IOSR-JDMS)
e-ISSN: 2279-0853, p-ISSN: 2279-0861.Volume 14, Issue 9 Ver. II (Sep. 2015), PP 63-68
www.iosrjournals.org

Thoracic Manifestations of Sarcoidosis Using Multi-Slice CT

Maged A. H. Shouker[1*], MD. Maged M. Ghanem[1], MD. Abdelsalam A. Elashry[2], MD. Khaled S. A. Karam[1], MD. Ahmed T. Shaarawy, MD[3]. Ahmad M. Ibraheem[4], MD.

[1]*Diagnostic Radiology department, El-Azhar Faculty of medicine. Cairo. Egypt.*
[2]*Diagnostic Radiology department, El-Azhar Faculty of medicine. Assiut. Egypt.*
[3]*Chest Disease Department, El-Azhar Faculty of medicine. Cairo. Egypt.*
[4]*Rheumatology department, Al-Azhar Faculty of medicine, Assiut. Egypt*

Aim: *The study was performed to define the prevalence and criteria of pulmonary lesions in patients with established diagnosis of sarcoidosis. We aim achieve criteria for rapid accurate diagnosis of sarcoidosis for favor of early proper treatment and good out come*

Methods: *This is a retrospective chart review study based on revision of the CT studies of (54) patients with established diagnosis of sarcoidosis to identify the related thoracic manifestations. The percentage for each finding is calculated. The lesions distribution is also defined. Accurate criteria for pulmonary sarcoidosis are defined.*

Results: *From the total reviewed 54 CT examinations 48 patients (88%) revealed variable patterns and degrees of pulmonary parenchyma changes and lymphadenopathy. 36 patients show typical bilateral hilar lymphadenopathy. The pulmonary micro-nodules were seen in 41 patients representing about 76% and were the predominant pattern in 35 patients (64%). The pulmonary nodules were predominantly peripheral, upper and mid zones and show predominant peri-lymphatic distribution. The peri-hilar consolidation opacities are seen at 3 patients. Two patients with miliary nodules pattern were detected. The ground glass attenuation is seen in 19 patients representing 35% of the population study and was predominate in 7 patients (13%). The detected pulmonary GGOs show no significant location predilection. Seven patients show changes of lung fibrosis which is predominantly seen in upper zones. .*

Conclusion: *The most predominant finding is micro-nodules in upper and mid-zones location, and peri-lymphatic distribution. The typical bilateral hilar lymphadenopathy is also predominant findings. The peri-hilar opacities despite not frequent but are specific.*

Key words: *Pulmonary sarcoidosis. Multi-slice CT. Micro-nodules. GGOs.*

I. Introduction

Sarcoidosis is a systemic disorder of unknown cause that is characterized by non-caseating granulomas with proliferation of epithelioid cells. Sarcoidosis commonly affects young and middle aged patients, with a slightly higher prevalence in women. The disease has distinct geographic and racial predilections, with African-Americans, Swedes, and Danes appearing to be most commonly affected *(1)*.

Clinical signs and symptoms are nonspecific and include fatigue, weight loss, general malaise, and, less commonly, fever. About one-half of patients remain asymptomatic.

Bilateral hilar lymphadenopathy is the most common radiologic finding. Adenopathy in the right paratracheal nodes, left aortic-pulmonary window, and subcarinal nodes can also be seen, often with associated pulmonary infiltrates *(1)*.

However, extrathoracic involvement can be an initial manifestation in one-half of symptomatic patients. Although skin and ocular lesions are common, the liver, spleen, lymph nodes, parotid glands, central nervous system (CNS), genitourinary system, muscles, and bones may also be involved *(2)*.

Thoracic radiologic abnormalities are seen at some stage in approximately 90% of patients with sarcoidosis, and an estimated 20% develop chronic lung disease leading to pulmonary fibrosis *(3)*.

At high-resolution CT, the most typical findings of pulmonary involvement are micronodules, fibrotic changes, and bilateral perihilar opacities. Atypical manifestations, such as mass like or alveolar opacities, honeycomb-like cysts, miliary opacities, mosaic attenuation, tracheobronchial involvement, and pleural disease, and complications such as aspergillomas, also may be seen *(3)*.

The diagnosis of sarcoidosis is commonly established on the basis of clinical and radiologic findings supported by histologic findings. Lung biopsy specimens can be obtained with transbronchial biopsy or from extrapulmonary sites such as the cervical lymph nodes and liver. Pathologic findings in sarcoidosis consist of noncaseating granulomas with epithelioid cells and large, multinucleated giant cells *(3)*.

Laboratory data show that the angiotensin-converting enzyme (ACE) level is commonly elevated and may correlate with disease activity. The CD4:CD8 ratio in the blood serum is commonly decreased. These abnormalities are helpful in making the diagnosis of sarcoidosis, although they may also be seen in other granulomatous diseases. Hypercalcemia is occasionally seen *(2).*

II. Materials and Methods

Consecutive patients with established diagnosis of sarcoidosis who were referred to our hospital between February 2009 and June 2012 were retrospectively studied. The diagnosis of the patients was based on non-caseating granulomas at histopathology assessment of biopsy specimens. A total of 54 patients satisfied the diagnostic criteria of sarcoidosis on histopathology basis and were rolled in this study**.**

CT Scanning Technique

All patients underwent HRCT pre and post non-ionic contrast axial slices with coronal and sagittal reformatted images. The scanner is Light speed 16 slice GE Medical Systems, Milwaukee, Wis. The slice thickness is 1.25 mm, and the interval 0.5 mm. Images were reconstructed with a high-spatial-frequency algorithm and displayed at window settings appropriate for viewing lung parenchyma (window center, -600 HU; window width, 1,500 HU) and for mediastinum.

Image analysis:

CT scans were reviewed by the authors. The Scans were reviewed at the axial, sagittal and coronal images in both lung and mediastinal window settings. The following features were analyzed.

First, the prevalence of thoracic changes is described in terms of number and percentage.

Second, the overall extent of lung disease was estimated to the nearest 10 % of lung segments involvement.

Third, the predominant pattern of lung disease made up of micro- nodules, ground-glass opacities (GGOs), and fibrosis with honey-combing were analyzed. Other non-common findings are described.

Fourth, the predominant zonal anatomic location of each pulmonary finding is described in terms of central or peripheral; upper, mid or lower zonal; anterior or posterior.

Fifth, the pattern distribution is described in the terms of centrilobular, perilymphatic or alveolar.

Statistical Analysis:

The percentages of each pattern and thoracic CT findings are calculated, and the predominant pattern is detected.

III. Results:

From the total reviewed 54 CT examinations, 6 revealed no abnormalities while 48 patients (88.9%) revealed variable patterns and degrees of pulmonary parenchymal changes and lymphadenopathy.

Thirty six patients (66%) of the study population showed typical bilateral hilar lymphadenopathy (Figure 1), while two cases (3.5%) showed lymphadenopathy at atypical other locations, i.e. left para-tracheal. From those 38 patients, 3 cases showed no associated parenchymal changes.

The pulmonary micro-nodules were seen in 41 patients representing about 76%. (Figure 2)

The peri-hilar consolidation opacities are seen at 3 patients (5.5%) associated with micro-nodules. (Figure 2)

Air space consolidations (Figure 3) and mass like lesions (Figure 4) were seen in four patients (7.4%) in association with micro-nodules.

Two patients with miliary nodules pattern were detected.

The ground glass attenuation is seen in 19 patients representing 35% of the population study. (Figure 5)

Seven patients (13%) showed changes of lung fibrosis. (Figure 6)

Twenty eight patients (52%) showed less than 50% extent of pulmonary changes, with details shown in table 1.

The pulmonary nodules were predominant in 35 patients (64%), while the ground glass opacities predominated in 7 (13%) patients.

The fibrotic changes and honey-combing were predominant in 3 patients (5 %).

The detected pulmonary nodules were predominantly peripheral, in the upper and mid zones. No significant predilection for anterior and posterior locations. The following table (2) describes the detailed distribution of pulmonary micro-nodules.

The detected pulmonary GGOs showed no significant location predilection.

The fibrotic changes were predominantly seen in upper zones.

There were no statistically significant differences between the distributions of micro-nodules pattern as regard the patient gender.

The micro-nodules showed predominant peri-lymphatic distribution seen in all cases.

Table (1) shows the extent of pulmonary changes

Extent of pulmonary changes (%)	Patient No.
10-29	16
30-49	12
50-69	11
>70	6
Total	45

Table (2) shows the location of pulmonary micro-nodules.

Distribution	Micro-nodules.
Central	14
Peripheral	27
Upper	21
Mid	14
Lower	6
Anterior	19
Posterior	22

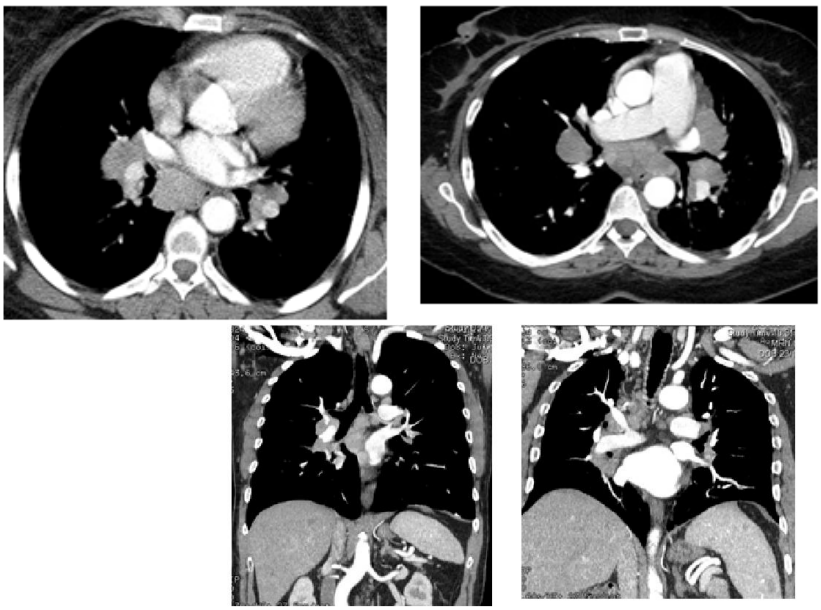

Figure 1: Direct Axial and coronal reformatted CT images of the chest with contrast in mediastinal window revealed multiple enlarged lymph nodes at the hilar and mediastinal groups.

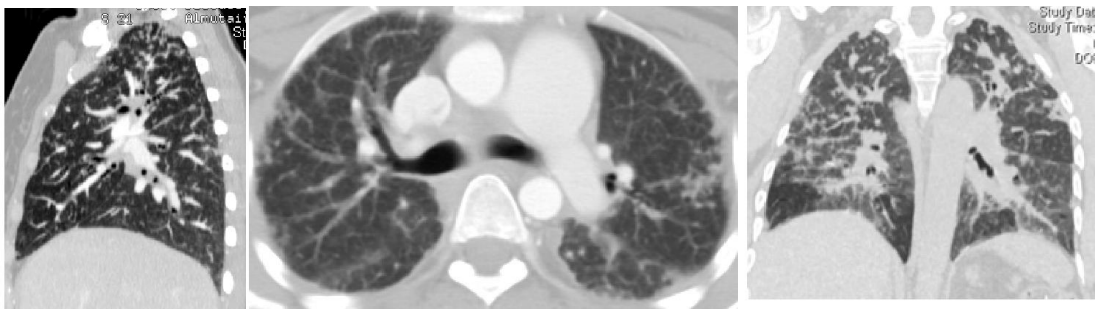

Figure 2: Sagittal, Axial and Coronal CT and HRCT showing micro-nodules and associated peri-hilar opacities.

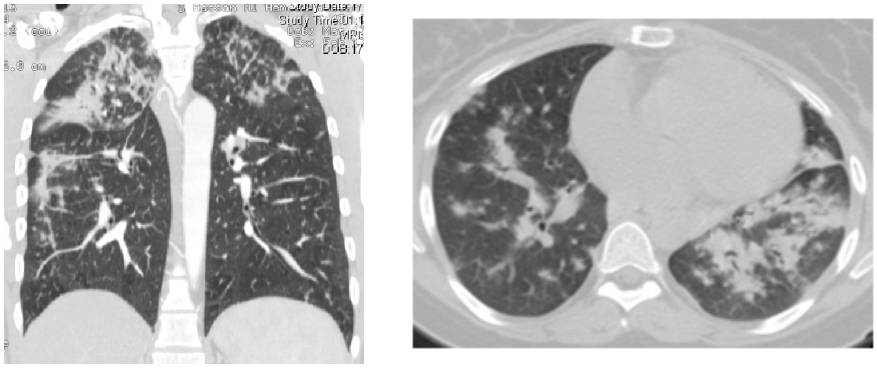

Figure 3: Coronal and Axial HRCT and CT showing Consolidation changes with micro-nodules.

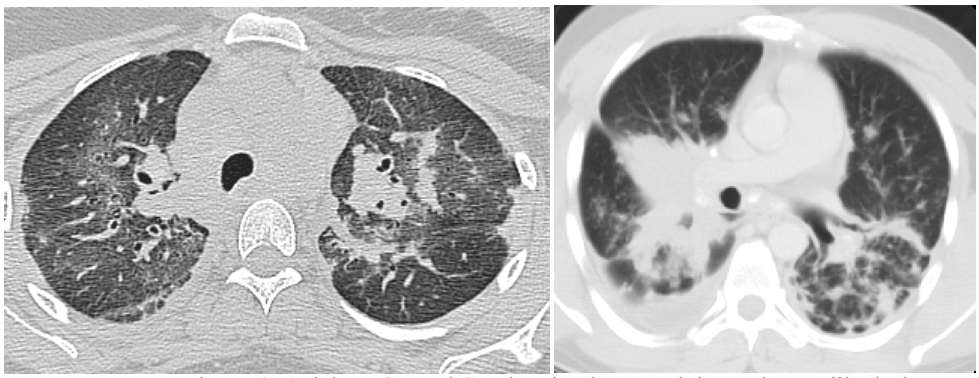

Figure 4: Axial HRCT and CT showing large nodules and mass like lesions.

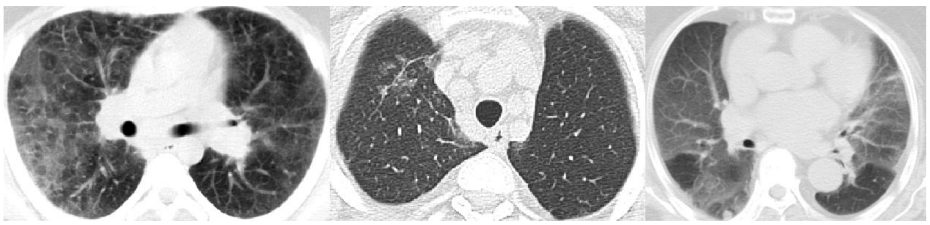

Figure 5: Direct Axial CT and HRCT images of the lungs in different patients with sarcoidosis displayed in lung window revealed nodular and patchy ground glass attenuation of the lungs.

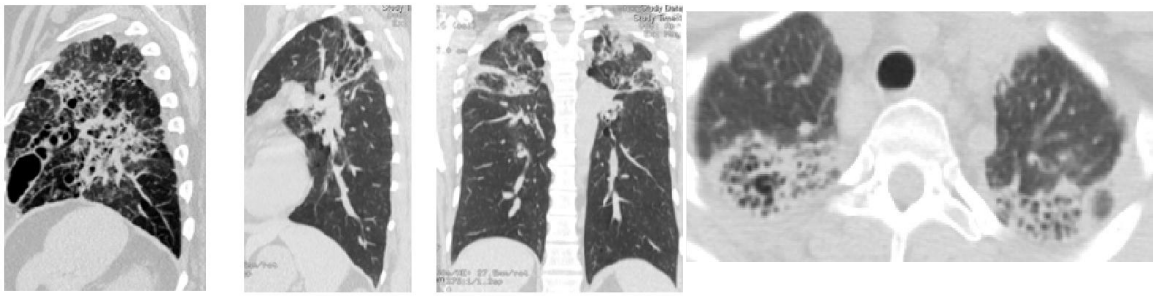

Figure 6: Sagittal, coronal and Axial CT images of the lungs in different patients with sarcoidosis displayed in lung window and high resolution revealed variable degrees and locations of pulmonary parenchymal fibrosis.

IV. Discussion

Involvement of the lung and the mediastinal and hilar lymph nodes in sarcoidosis is most common, being seen in approximately 90% of patients, and accounts for most of the morbidity and mortality associated with the condition (1).

Pulmonary function tests typically demonstrate a restrictive ventilation defect with decreased volumes and decreased carbon monoxide diffusing capacity. These functional alterations tend to become more frequent and marked from stage 1 to stage 4 (4).

The Siltzbach classification system defines the following five stages of sarcoidosis based on radiographic findings: stage 0, with a normal appearance at chest radiography; stage 1, with lymphadenopathy only; stage 2, with lymphadenopathy and parenchymal lung disease; stage 3, with parenchymal lung disease only; and stage 4, with pulmonary fibrosis (5).

Factors associated with a poor prognosis include stage 2 or 3 pulmonary disease at the time of initial diagnosis, disease onset after the age of 40 years, black race (5), hypercalcemia, splenomegaly, and osseous involvement (6).

A diagnosis of sarcoidosis is established on the basis of compatible clinical and radiologic findings and histologic evidence of the presence of noncaseous epithelioid cell granulomas in one or more organs and the absence of causative organisms or particulates (7).

The imaging features of sarcoidosis are protean and can be shown with a variety of imaging techniques. Diagnostic imaging can help in monitoring therapeutic response in symptomatic patients (8).

High-resolution CT has proved superior to conventional CT for assessing subtle parenchymal details and discriminating between inflammation and fibrosis in patients with pulmonary sarcoidosis (9).

The thin-section collimation (1- to 1.5- mm section thickness) and high-spatial-frequency reconstruction algorithms that are used to generate high-resolution CT images allow improved detection of nodular and reticular opacities, thickened interlobular septa, and faint ground-glass opacities, making the technique especially useful for identifying and managing sarcoidosis (10).

High-resolution CT may be particularly helpful for distinguishing active inflammation from irreversible fibrosis in selected patients with stage 2 or 3 sarcoidosis. Nodules, ground-glass opacities, and alveolar opacities are suggestive of granulomatous inflammation that may be reversed with therapy (11). By contrast, honeycomb-like cysts, bullae, broad and coarse septal bands, architectural distortion, volume loss, and traction bronchiectasis are indicative of irreversible fibrosis (7).

The most common pattern is well-defined, bilateral, symmetric hilar and right paratracheal lymph node enlargement. Bilateral hilar lymph node enlargement, alone or in combination with mediastinal lymph node enlargement, occurs in an estimated 95% of patients affected with sarcoidosis (12).

Middle mediastinal nodes (at the left paratracheal level, subcarinal level, and level of the aortopulmonary window), prevascular nodes, or both are involved in approximately 50% of patients (9).

Mediastinaladenopathy without hilar involvement is rare and is more frequently seen in older patients (2). Occasionally, calcification occurs in affected nodes. Calcification can be amorphous, punctate, or eggshell-like. It suggests a chronic condition (2).

This study revealed that 70% of patients had thoracic lymphadenopathy and the majority of the enlarged nodes are seen at the hilar groups, findings which correlate with other studies.

A perilymphatic distribution of micronodular lesions is the most common parenchymal disease pattern seen in patients with pulmonary sarcoidosis (75%–90% of cases). High-resolution CT shows sharply defined, small, rounded nodules, usually with a bilateral and symmetric distribution, predominantly in the upper and middle zones. The nodules are found most often in the sub-pleural peri-bronchovascularinterstitium and less often in the interlobular septa (3).

The micro-nodules represented 76% in our study and were the predominant finding in 64% of our study population. All the cases showed peri-lymphatic distribution of nodules.

The predominant locations in our study were the peripheral, sub-pleural, upper and mid-zones. No statistically significant differences were present between the anterior and posterior locations.

Four cases (7.5%) showed consolidations and mass like lesions in association with micro-nodules.

Pulmonary masses were seen in 15%–25% of patients with parenchymal opacities. At CT, they usually appear as ill-defined irregular opacities measuring 1–4 cm in diameter that represent coalescent interstitial granulomas (3).

Consolidation was seen in 10%–20% of patients with sarcoidosis. It is usually bilateral and symmetric and predominantly involving the peribronchovascular regions of the middle and upper zones of the lungs. These regions of consolidation, which may contain air bronchograms, commonly have ill-defined margins, as consolidation “fades” to a nodular pattern toward the lung periphery. Consolidation in sarcoidosis reflects the confluence of numerous micro-nodules (3).

Confluent nodular opacities that appear on CT images as bilateral areas of lung consolidation with irregular edges and blurred margins, radiating from the hilum toward the periphery, are often seen with or without air bronchogram. These areas of consolidation are less homogeneous peripherally and are usually accompanied by micro-nodules (13).

The peri-hilar opacity pattern is seen in 5% of our study population.

The miliary Opacities are rare in sarcoidosis (<1% of cases), and its appearance at imaging may warrant the inclusion of entities such as tuberculosis, pneumoconiosis, and metastatic lesions in the differential diagnosis. (3).

Two patients (3.7%) with miliary nodules were seen at our study.

Patchy ground-glass opacities are seen in an estimated 40% of patients with parenchymal changes due to pulmonary sarcoidosis; extensive ground-glass opacities are much less common (3).

The GGOs were seen in 35% at our study and are the predominant findings in 13% of our study patients.

This is in agreement with the findings of Eva Criado who stated that patchy ground-glass opacities in sarcoidosis are always accompanied by other abnormalities and often are superimposed on a background of interstitial nodules (3).

Fibrotic and cystic lesions typically involve the upper and middle lung zones and follow the large airways in a perihilar distribution. Posterior displacement of the main or upper-lobe bronchus and volume loss (particularly in the upper lobes) are characteristic features of chronic fibrosis (3).

Thirteen % of this study population showed fibrotic changes in the form of fibrotic bands and cystic changes with predominant upper and mid zones locations.

V. Conclusion:

The most predominant finding was micro-nodules in upper and mid-zones location, and peri-lymphatic distribution. The typical bilateral hilar lymphadenopathy was also a predominant finding. The peri-hilar opacities despite not frequent but are specific. The GGOs don't stand alone as a strong diagnostic finding, but is frequently seen.

References

[1]. Statement on sarcoidosis: Joint Statement Committee, February 1999. Am J RespirCrit Care Med 1999; 160:736–755.

[2]. Takashi Koyama, MD. Hiroyuki Ueda, MD.Kaori Togashi, MD. Radiologic Manifestations of Sarcoidosis in Various Organs.RadioGraphics 2004; 24:87–104

[3]. Eva Criado, MD. Marcelo Sánchez, MD. José Ramírez, MD, PhD Pedro Arguis, MD. Pulmonary Sarcoidosis: Typical and Atypical Manifestations at High- Resolution CT with Pathologic Correlation.RadioGraphics 2010; 30:1567–1586.

[4]. Lynch JP 3rd, White ES. Pulmonary sarcoidosis.EurRespirMonogr 2005;10:105–129.

[5]. Siltzbach LE, James DG, Neville E. Course and prognosis of sarcoidosis around the world. Am J Med 1974; 57(6):847–852.

[6]. Neville E, Walker AN, James DG. Prognostic factors predicting the outcome of sarcoidosis: an analysis of 818 patients. Q J Med 1983; 52(208):525–533.

[7]. Baughman RP, Winget DB, Bowen EH, Lower EE. Predicting respiratory failure in sarcoidosis patients.SarcoidosisVasc Diffuse Lung Dis 1997; 14(2): 154–158.

[8]. Hima B. Prabhakar1, Chad B. Rabinowitz1, Fiona K. Gibbons2. Imaging Features of Sarcoidosis on MDCT, FDG PET, and PET/CT. AJR: 190 March 2008.

[9]. Brauner MW, Grenier P, Mompoint D, Lenoir S, de Crémoux H. Pulmonary sarcoidosis: evaluation with high-resolution CT. Radiology 1989;172(2): 467–471.

[10]. Nishimura K, Itoh H, Kitaichi M, Nagai S, Izumi T. CT and pathological correlation of pulmonary sarcoidosis. Semin Ultrasound CT MR 1995; 16(5): 361–370.

[11]. Müller NL, Miller RR. Ground-glass attenuation, nodules, alveolitis, and sarcoid granulomas.Radi-ology 1993; 189(1):31–32.

[12]. Reich JM. Mortality of intrathoracicsarcoidosis in referral vs population-based settings: influence of stage, ethnicity, and corticosteroid therapy. Chest 2002; 121(1):32–39.

[13]. Abehsera M, Valeyre D, Grenier P, Jaillet H, Battesti JP, Brauner MW. Sarcoidosis with pulmonary fibrosis: CT patterns and correlation with pulmonary function. AJR Am J Roentgenol 2000; 174(6): 1751–1757.